Peptide fragments of the dihydropyridine receptor can modulate cardiac ryanodine receptor channel activity and sarcoplasmic reticulum Ca^{2+} release

Angela F. DULHUNTY*[1], Suzanne M. CURTIS*, Louise CENGIA†, Magdalena SAKOWSKA* and Marco G. CASAROTTO‡

*John Curtin School of Medical Research, Australian National University, Canberra, ACT 2601, Australia, †Biotron Ltd, Australian National University, ACT 2601, Australia, and ‡Research School of Chemistry, Australian National University, Canberra, ACT 2601, Australia

We show that peptide fragments of the dihydropyridine receptor II–III loop alter cardiac RyR (ryanodine receptor) channel activity in a cytoplasmic Ca^{2+}-dependent manner. The peptides were A_C (Thr-793–Ala-812 of the cardiac dihydropyridine receptor), A_S (Thr-671–Leu-690 of the skeletal dihydropyridine receptor), and a modified A_S peptide [*A_S(D-R18)*], with an extended helical structure. The peptides added to the cytoplasmic side of channels in lipid bilayers at $\geqslant 10$ nM activated channels when the cytoplasmic [Ca^{2+}] was 100 nM, but either inhibited or did not affect channel activity when the cytoplasmic [Ca^{2+}] was 10 or 100 μM. Both activation and inhibition were independent of bilayer potential. Activation by A_S, but not by A_C or *A_S(D-R18)*, was reduced at peptide concentrations > 1 μM in a voltage-dependent manner (at $+40$ mV). In control experiments, channels were not activated by the scrambled A_S sequence (*A_SS*) or skeletal II–III loop peptide (*NB*). Resting Ca^{2+} release from cardiac sarcoplasmic reticulum was not altered by peptide A_C, but Ca^{2+}-induced Ca^{2+} release was depressed. Resting and Ca^{2+}-induced Ca^{2+} release were enhanced by both the native and modified A_S peptides. NMR revealed (i) that the structure of peptide *A_S(D-R18)* is not influenced by [Ca^{2+}] and (ii) that peptide A_C adopts a helical structure, particularly in the region containing positively charged residues. This is the first report of specific functional interactions between dihydropyridine receptor *A* region peptides and cardiac RyR ion channels in lipid bilayers.

Key words: cardiac ryanodine receptor activity, dihydropyridine receptor, muscle contraction, ryanodine receptor probe.

INTRODUCTION

The RyR (ryanodine receptor) Ca^{2+}-release channel is located in the SR (sarcoplasmic reticulum) of striated muscle fibres. The Ca^{2+} required for muscle contraction is released from Ca^{2+} stores in the terminal cisternae of the SR through RyR channels. During EC (excitation–contraction) coupling, the cardiac RyR is activated by a Ca^{2+} influx through L-type Ca^{2+} channels [DHPRs (dihydropyridine receptors)], via Ca^{2+}-induced Ca^{2+} release. In contrast in skeletal muscle, RyR1 is thought to be activated during EC coupling by a protein–protein interaction with DHPR, not by Ca^{2+}-induced Ca^{2+} release. The II–III loop between the second and third repeats of the DHPR, with the skeletal sequence between Leu-720 and Leu-764, is required for skeletal-type EC coupling, which is independent of Ca^{2+} influx through the DHPR [1–3].

Because of its central role in EC coupling, the RyR is a useful pharmacological target for modulating muscle contraction and RyR-active compounds such as caffeine, ryanodine, dantrolene and cADP ribose are frequently used in this capacity [4]. Peptides derived from the ***A*** region (residues Thr-671–Leu-690) of the II–III loop of the skeletal muscle DHPR provide a new class of compounds that interact with RyR channels. These peptides (at $\geqslant 1$ μM) enter the pore from the cytoplasm and block skeletal RyR channels at positive membrane potentials, when current flows from the cytoplasmic to the luminal side of the channel [5,6]. The peptides are effective activators of skeletal muscle RyRs at lower concentrations (1–100 nM) and have been used in this capacity to probe skeletal muscle RyR activity [7–10]. The same peptides have been found to be ineffective in activating cardiac RyRs [11,12]. This inability to activate cardiac RyRs is surprising for several reasons. Firstly, a scorpion toxin (imperatoxin A) that is thought to bind to the same site as the skeletal *A* peptide acts on both cardiac and skeletal RyRs [6,13–15]. Secondly, the recombinant skeletal DHPR II–III loop binds to cardiac RyRs in a two-hybrid system [16] and the skeletal *A* peptide binds to cardiac RyRs in surface plasmon resonance [17]. Since these observations show that skeletal DHPR fragments bind to cardiac RyRs, we have further investigated the functional effects of the skeletal DHPR *A* fragments on cardiac RyR channels. The actions of the cardiac *A* fragment have also been examined, since the C-terminal 10 residues of this peptide reduce Ca^{2+} spark frequency in cardiac myocytes [18].

We find that the *A* fragments of both skeletal and cardiac DHPR, as well as modified skeletal *A* fragments, alter cardiac RyR activity in a [Ca^{2+}]-dependent manner. The peptides activate cardiac RyR channels when the cytoplasmic [Ca^{2+}] is sub-activating (100 nM), but inhibit channels that are activated by 10–100 μM Ca^{2+}. Both these effects of the peptides are voltage-independent. The inhibition of the channel at activating Ca^{2+} is distinctly different from a voltage-dependent block seen only at positive potentials and only with the native skeletal *A* fragment. The cardiac DHPR *A* fragment depressed Ca^{2+}-induced Ca^{2+} release from cardiac SR, whereas the skeletal DHPR *A* fragments enhanced both resting and Ca^{2+}-induced Ca^{2+} release. The activating effects of the *A* peptides

Abbreviations used: RyR, ryanodine receptor; SR, sarcoplasmic reticulum; EC, excitation–contraction; DHPR, dihydropyridine receptor; BAPTA, bis-(*o*-aminophenoxy)ethane-*N*,*N*,*N*′,*N*′-tetra-acetic acid; NOESY, nuclear Overhauser enhancement spectroscopy.

[1] To whom correspondence should be addressed, at PO Box 334, Canberra, ACT 2601, Australia (e-mail angela.dulhunty@anu.edu.au).

Table 1 Effect of adding 2 mM MgATP to native cardiac RyRs in the presence of 10^{-7} or 10^{-4} M *cis* Ca^{2+} at + 40 or − 40 mV

Data are given for open probability (P_o), mean open time (T_o) and mean closed time (T_c), before (initial) and after (MgATP) addition of MgATP. Data in italics show a significant change upon addition of 2 mM MgATP. Asterisks indicate a significant difference between data with 10^{-7} M *cis* Ca^{2+} and 10^{-4} M *cis* Ca^{2+}.

		+ 40 mV		− 40 mV	
cis [Ca^{2+}]		10^{-7} M ($n = 7$)	10^{-4} M ($n = 10$)	10^{-7} M ($n = 7$)	10^{-4} M ($n = 10$)
P_o	Initial	0.004 ± 0.002	0.25 ± 0.08*	0.004 ± 0.001	0.17 ± 0.08*
	MgATP	*0.038 ± 0.022*	*0.40 ± 0.11**	*0.029 ± 0.016*	*0.38 ± 0.09**
T_o (ms)	Initial	2.21 ± 0.34	26.2 ± 22.4	2.3 ± 0.34	22.8 ± 20.3
	MgATP	*2.83 ± 0.35*	*45.6 ± 20.1**	2.6 ± 0.30	26.9 ± 15.3*
T_c (ms)	Initial	1084 ± 313	142 ± 56.2*	918 ± 188	161 ± 57*
	MgATP	*308 ± 114*	76 ± 30.5	686 ± 272	*67 ± 47**

may not have been reported previously because (i) it would not have been seen with activating cytoplasmic Ca^{2+} concentrations used in previous single-channel experiments [12] and (ii) it is most prominent in enhancing Ca^{2+}-induced Ca^{2+} release from cardiac SR, but only resting Ca^{2+} has been examined previously. We conclude that these DHPR fragments corresponding to the skeletal and cardiac DHPR *A* region bind to the cardiac RyR, alter its activity under appropriate conditions, and can therefore be used as probes for cardiac as well as skeletal RyR function.

EXPERIMENTAL

Materials

The following peptides were synthesized [5,19,20]. Peptide A_S, ^{671}TSAQKAKAEERKRRKMSRGL^{690}; peptide A_C, ^{793}TSAQKEEEEEKERKKLARTA^{812}; peptide *NB*, ^{689}GLPNKTEEEKSVMAKKLEQL^{708}; peptide A_SS, TRKSRLARGQKAKAKSEMRG.

Isolation of SR vesicles

The techniques were modified from Chamberlain and Fleischer [21] as described in [22]. Crude microsmal vesicles were suspended in buffer containing 290 mM sucrose, 10 mM imidazole (pH 6.9 with HCl), 0.5 mM dithiothreitol, 3 mM sodium azide and 650 mM KCl, plus protease inhibitors (2.2 μM leupeptin, 1 μM pepstatin A, 1 mM benzamidine and 0.5 mM PMSF in DMSO). The crude vesicles were snap-frozen and stored either in liquid N_2 or at − 70 °C.

Single-channel measurements [5,19,20]

Recording solutions were (*cis*) 230 mM caesium methanesulphonate, 20 mM CsCl and 10 mM Tes (pH 7.4 with CsOH) and (*trans*): 230 mM caesium methanesulphonate, 20 mM CsCl, 1 mM $CaCl_2$ and 10 mM Tes (pH 7.4). The *cis* Ca^{2+} concentration was buffered to 10^{-7} M using 2 mM BAPTA [bis-(*o*-aminophenoxy)ethane-*N*,*N*,*N*′,*N*′-tetra-acetic acid], or to 10^{-6} and 10^{-5} M using a mixture of 2 mM BAPTA plus 2 mM dibromoBAPTA. The free Ca^{2+} concentration was measured with a Ca^{2+}-sensitive electrode. The *cis* chamber was held at ground and the voltage of the *trans* chamber controlled. Bilayer potential, expressed as $V_{cis} - V_{trans}$, was changed every 30 s between + 40 and − 40 mV. We recorded 2 min of activity under control conditions and after each addition of peptide. Baseline drift in channel records was corrected before analysis using an in-house program, Baseline, developed by Dr D. R. Laver. Channel analysis was performed using Channel 2 (developed by P. W. Gage and M. Smith, John Curtin School of Medical Research, Australian National University, Canberra, Australia). The mean current (I′; an average of all data points in the record) was calculated. This measure was applied to single- and multiple-channel recordings and included openings to all conductance levels. A 'threshold' analysis was used to determine single-channel characteristics in records in which one channel only was active (i.e. the maximum current was no greater than the maximum single-channel opening). Open probability (P_o) and mean open or closed times (T_o or T_C) were obtained from the intervals between the current crossing a threshold level set at approx. ± 3 pA from the baseline. For each experiment, I′ and single-channel parameters were obtained from 30 s of continuous channel recording in the absence of peptide and then with increasing concentrations of peptide. Vesicles from six different sheep ventricles were used to obtain data.

Ca^{2+} release

SR vesicles (100 μg/ml) were added to a solution containing 100 mM KH_2PO_4 (pH 7), 4 mM $MgCl_2$, 1 mM Na_2ATP and 0.5 mM antipyrylazo III. The method previously used with skeletal SR vesicles [5] was modified for cardiac SR by (i) adding an ATP-regenerating system – phospho(enol)pyruvate (5 mM) and pyruvate kinase (25 μg/ml) – to the solution, and (ii) a period of 3 min was allowed for loading after each addition of Ca^{2+}. Extravesicular [Ca^{2+}] was monitored at 710 nm. Vesicles were loaded with Ca^{2+} by adding four aliquots of $CaCl_2$, each initially increasing the extravesicular Ca^{2+} concentration by 7.5 μM. Then thapsigargin (200 nM) was added to block the Ca^{2+} ATPase. Ca^{2+} release with thapsigargin was subtracted from the initial rates of release with activating agents. Addition of Ruthenium Red (4–5 μM) confirmed that Ca^{2+} release was through the RyR. The Ca^{2+} ionophore A23187 (3 μg/ml) was added to measure the Ca^{2+} remaining in the vesicles at the end of each experiment.

Ca^{2+} uptake

Ca^{2+} uptake was measured under the same conditions as Ca^{2+} release (above) except that Ruthenium Red was added at the start of the experiment to suppress any Ca^{2+} leak through the RyR. The rate of Ca^{2+} uptake was measured from the initial slope of the decline in [Ca^{2+}] following the addition of 7.5 μM Ca^{2+} to the extravesicular solution.

NMR spectroscopy

Peptide A_C was dissolved in 10 % ^2H_2O/90 % H_2O to a final concentration of approx. 2 mM at pH 5.0. Peptide A_S*(D-R18)* was

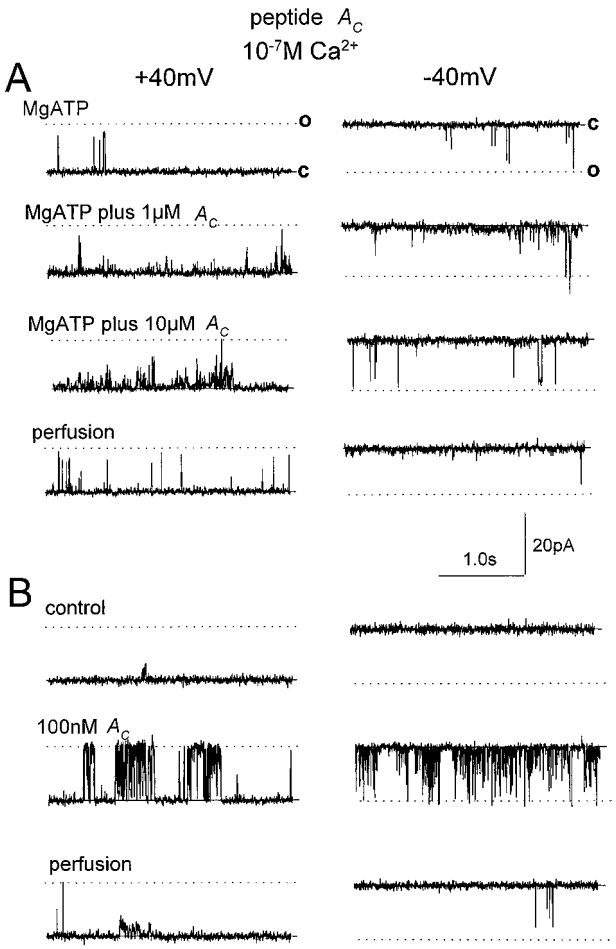

Figure 1 Peptide A_C reversibly activates single cardiac RyR channels at sub-activating *cis* [Ca^{2+}]

Channel opening (this and subsequent figures) is upwards at + 40 mV (left) and downwards at − 40 mV (right), from the closed level (c) to the maximum single channel current (o). (**A**) Sequential records of control activity with 2 mM MgATP in the *cis* chamber (first trace), after addition of 1 μM (second trace) then 10 μM peptide (third trace), and after *cis* perfusion with a 100 nM Ca^{2+} solution lacking MgATP and peptide (fourth trace). Similar results were obtained in seven experiments. (**B**) Sequential records of control activity (100 nM *cis* Ca^{2+}; first trace), after adding 100 nM A_C (second trace) and after perfusion (peptide reduced to approx. 30 pM; third trace). Reversibility was seen in five similar experiments.

dissolved at 2 mM in the *cis* bilayer solution (above). NMR spectroscopy was then performed as described previously [19,20].

Statistics

The significance of differences between values was tested using a Students *t* test, either one- or two-tailed, for independent or paired data as appropriate or by the non-parametric Sign test [23]. Differences were considered significant when $P \leqslant 0.05$. Data are shown as means $\pm$ 1 × S.E.M.

RESULTS

Peptides were added to the *cis* solution bathing the cytoplasmic side of native cardiac RyR channels. The channels were identified as RyRs by their Cs^+ conductance of approx. 250 pS (with 1 mM *trans* Ca^{2+}) and their block by 30 μM Ruthenium Red.

Table 2 Comparison of the open probability (P_o) of channels under initial conditions (in the absence of MgATP or peptide) with that after perfusion of the *cis* chamber with 10 vol. of solution lacking MgATP or peptide

Perfusion led to an approx. 3000-fold dilution of peptide A_C, from 100 μM to approx. 30 nM or peptide A_S from 50 μM to approx. 15 nM. Asterisks indicate that activity after perfusion was significantly higher than the initial activity of the channel after incorporation into the bilayer.

			P_o	
	n	Bilayer potential (mV)	Initial	Perfusion 30 s
Peptide A_C	6	+ 40	0.004 ± 0.002	0.028 ± 0.007*
cis Ca^{2+} (10^{-7} M)		− 40	0.002 ± 0.001	0.095 ± 0.057*
Peptide A_S	7	+ 40	0.047 ± 0.013	0.054 ± 0.029
cis Ca^{2+} (10^{-7} M)		− 40	0.056 ± 0.058	0.296 ± 0.118*

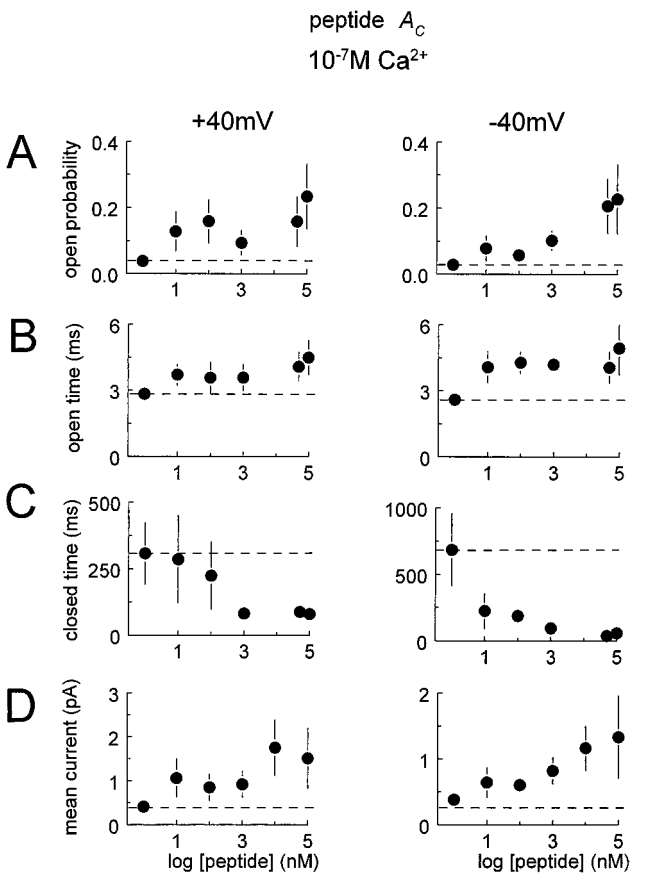

Figure 2 Peptide A_C increases the open probability and mean current of channels at sub-activating *cis* [Ca^{2+}] by shortening the closed durations

(**A**), (**B**) and (**C**) show average open probability, mean open time and mean closed time respectively, at + 40 mV (left) and − 40 mV (right). $n = 4$ for 10 nM peptide and $n = 6$ for > 10 nM peptide. (**D**) Mean current provides a threshold-independent measure of channel activity (see the Experimental section). The first symbol in these and subsequent similar graphs indicates control data.

Effects of the cardiac peptide, A_C, on cardiac RyR channels

MgATP was used to better reproduce *in vivo* conditions and its addition resulted in increased activity at both *cis* [Ca^{2+}]s (Table 1) as previously reported [24].

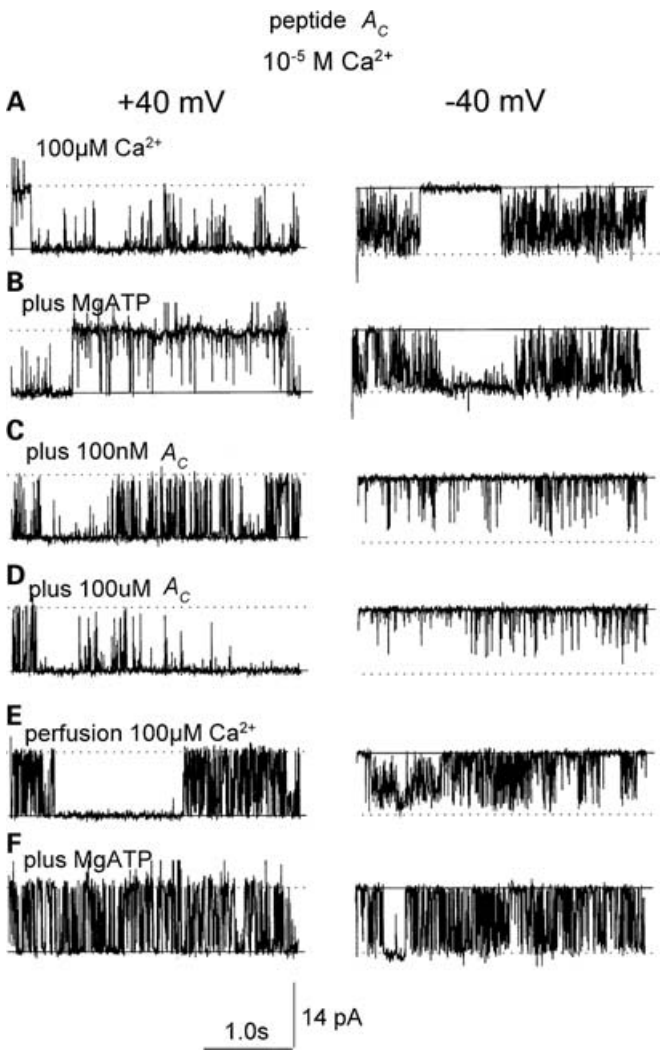

Figure 3 Peptide A_C causes reversible voltage-independent inhibition of cardiac RyR channels activated by 100 μM *cis* Ca^{2+}

Sequential records are shown at + 40 mV (left) and − 40 mV (right) (**A**; reading from the top), after adding 2 mM *cis* MgATP (**B**), then 100 nM A_C (**C**) and 100 μM A_C (**D**). Some recovery is seen after perfusion with the 100 μM Ca^{2+} solution, both before (**E**) and after (**F**) addition of 2 mM MgATP. The [peptide] after perfusion was approx. 30 nM and channel activity in (**E**) and (**F**) was less than under equivalent control conditions in (**A**) and (**B**) respectively, showing maintained inhibition with this low [peptide]. Similar results were obtained in seven experiments.

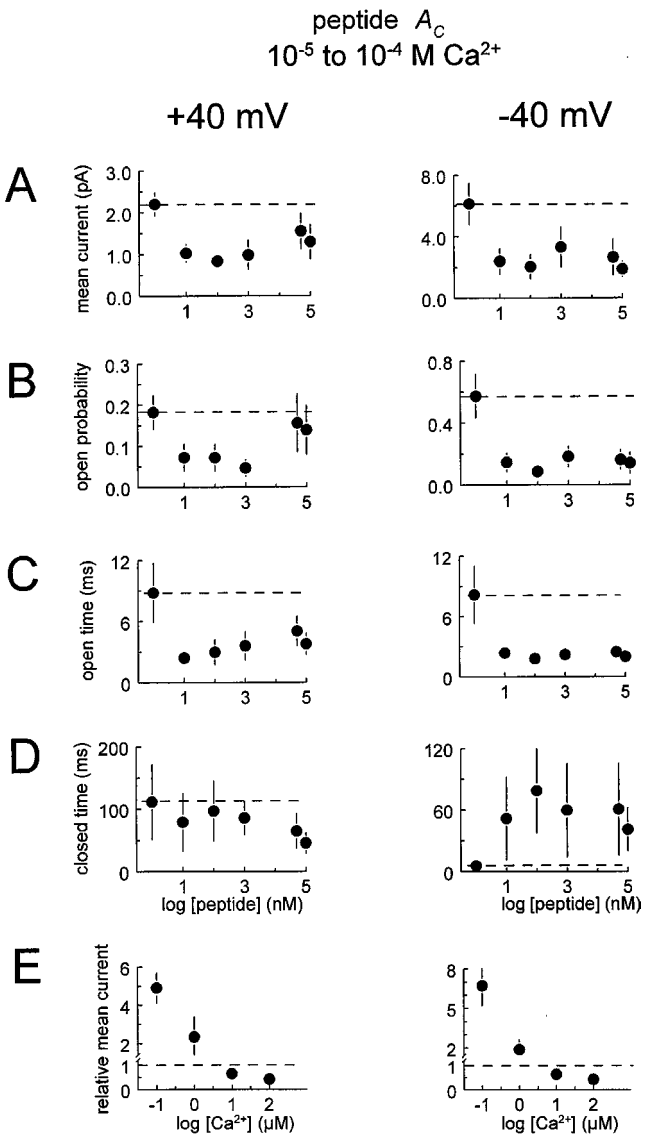

Figure 4 Peptide A_C reduces mean current and open probability of Ca^{2+}-activated channels by reducing the open duration

Average data are shown at + 40 and − 40 mV. (**A**) Mean current; (**B**) open probability; (**C**) mean open time; (**D**) mean closed time. $n = 8$ experiments for mean current, and $n = 5$ for threshold analysis. Parameter values with 10 μM ($n = 4$) and 100 μM *cis* Ca^{2+} ($n = 4$) were similar and have been combined in the average data. (**E**) Relative mean current in the presence of 1 μM peptide A_C as a function of *cis* [Ca^{2+}]. Numbers of experiments at 100 nM and 100 μM Ca^{2+} are given above. $n = 6$ for 1 μM Ca^{2+} and $n = 4$ for 10 μM Ca^{2+}.

Peptide A_C activates cardiac RyRs at resting cytoplasmic Ca^{2+} concentrations but inhibits channels that are Ca^{2+}-activated

Peptide A_C increased cardiac RyR activity when *cis* [Ca^{2+}] was 100 nM (Figure 1). Washout of 100 μM A_C and MgATP led to a fall in activity, due to dilution of ATP and peptide. Activity after washout was greater than the initial activity (Table 2), indicating that the peptide, although diluted, remained at an activating concentration and was effective in the virtual absence of MgATP. Reversible activation was seen when a lower concentration of 100 nM peptide A_C was used (Figure 1B).

Activation by peptide A_C was caused by a reduction in the time that the channel was closed (Figure 2). The similar changes in mean current and open probability show that the data was not substantially biased by exclusion of small-conductance openings (open probability analysis) or inclusion of multiple channel activity (mean current analysis).

In contrast to activation with 100 nM *cis* Ca^{2+}, reversible inhibition was seen when when peptide A_C was added to channels activated by *cis* [Ca^{2+}] of 10 or 100 μM (Figure 3). Perfusion of 100 μM peptide A_C from the *cis* chamber (with dilution to approx. 30 nM) was accompanied by some recovery of activity (Figure 3). The reduction in activity (mean current and open probability) was due to a decrease in the duration of the channel opening (Figure 4). The [Ca^{2+}]-dependence of the effect of peptide A_C (Figure 4E) shows that activation at 100 nM Ca^{2+} declines with 1 μM Ca^{2+} and that the effect of the peptide becomes inhibitory at 10 and 100 μM Ca^{2+}.

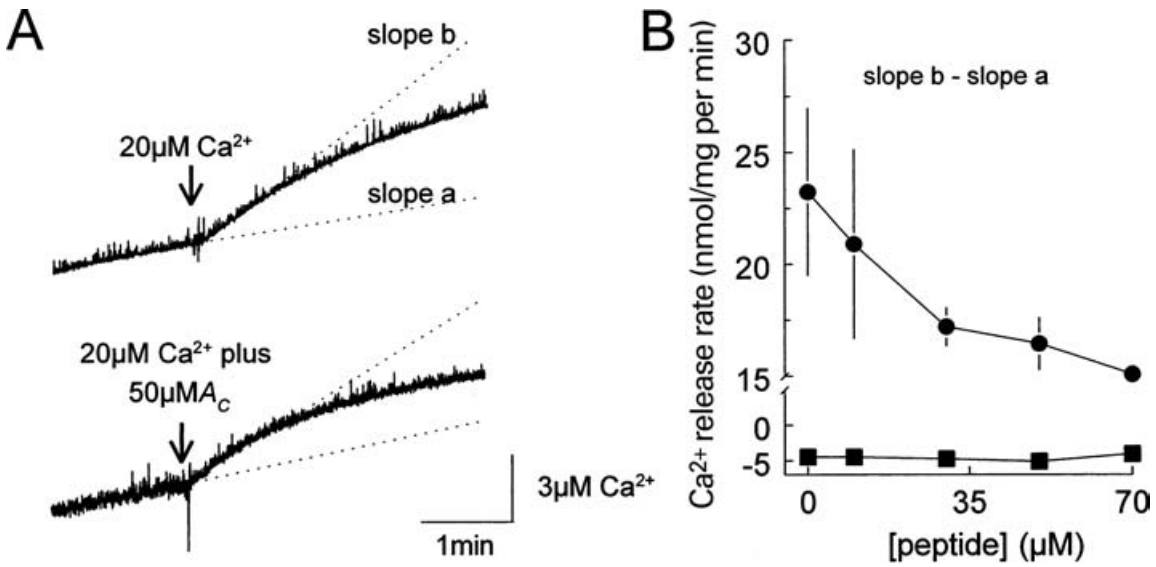

Figure 5 Peptide A_C reduces Ca^{2+}-induced Ca^{2+} release from cardiac SR, but not resting Ca^{2+} leak

(**A**) Changes in absorbance, reflecting changes in extravesicular [Ca^{2+}], in SR vesicles that have been partially loaded with Ca^{2+}. The initial part of each record shows resting Ca^{2+} leak after addition of thapsigargin. The arrow indicates addition of 20 μM Ca^{2+}, alone (upper) or with peptide A_C (lower). The step increase in absorbance with 20 μM Ca^{2+} has been subtracted. Broken lines indicate the release rate in thapsigargin (slope a), and after Ca^{2+}/peptide addition (slope b). (**B**) Shows Ca^{2+} release in nmol/mg of protein per min (b − a). ●, Ca^{2+}-induced Ca^{2+} release ($n = 3$); ■, individual measurements when peptide alone was added 3 min after thapsigargin.

Peptide A_C inhibits Ca^{2+}-induced Ca^{2+} release from cardiac SR vesicles

The inhibition of single Ca^{2+}-activated channels was reflected in the effect of peptide A_C on Ca^{2+} release from cardiac SR vesicles. The peptide had little effect on resting Ca^{2+} release, but reduced the rate of Ca^{2+}-induced Ca^{2+} release (Figure 5).

The effects of the native and modified skeletal peptide, A_S, on cardiac RyR channels

MgATP was omitted in experiments with peptide A_S because the peptide failed to activate pig skeletal RyRs in the presence of ATP [7]. However, since the peptide also interacted with channels in SR vesicles in the presence of MgATP (see below), the effects on the cardiac RyR were not ATP-dependent.

Biphasic activation of native peptide A_S on cardiac RyR channels at resting cytoplasmic [Ca^{2+}] and channel block at activating [Ca^{2+}]

Peptide A_S caused a reversible increase in channel activity when *cis* [Ca^{2+}] was 100 nM. Channel activation was greater at −40 mV than at +40 mV and there were more channel openings to submaximal conductance levels with 1 μM peptide A_S at +40 mV (Figure 6). The subconductance activity has been described with skeletal RyRs and attributed to pore block following binding of the basic peptide A_S to low-affinity acidic sites, located in the pore [5]. Average data showed a monophasic increase in activity at −40 mV, but biphasic increase at +40 mV, because higher concentrations of peptide blocked the channel (Figures 7A and 7B, ●). The increase in activity was caused by a substantial decrease in closed times (Figure 7D).

The ability of the peptide A_S to activate the RyR channel was substantially reduced with 100 *cis* μM Ca^{2+}. Although pore block at +40 mV was stronger at the higher *cis* [Ca^{2+}], activity at −40 mV was not significantly different from control (Figure 7, ○).

The [Ca^{2+}]-dependence of the effects of peptide A_S (Figure 7E) shows that, as with the cardiac peptide, activation was greatest with 100 nM *cis* Ca^{2+} and declined with increasing [Ca^{2+}].

Modified peptide A_S activates cardiac RyRs at resting Ca^{2+} concentrations, but inhibits Ca^{2+}-activated channels

The actions of peptide *A_S(D-R18)* were qualitatively similar to the Ca^{2+}-dependent and voltage-independent effects of peptides A_S and A_C. Activation by *A_S(D-R18)* with 100 nM *cis* [Ca^{2+}] was stronger than that with peptide A_C or peptide A_S, but, as with the other two peptides, was due to a decrease in channel closed times (Figures 8A–8D, ●). Conversely, voltage-independent inhibition in the presence of 100 μM *cis* [Ca^{2+}] was caused by an abbreviation of the open times (Figures 8A–8D, ○).

Voltage-dependent block of activity was not seen for *A_S(D-R18)* with 100 nM Ca^{2+}, and, if present with 100 μM Ca^{2+}, was masked by inhibition. The effects of *A_S(D-R18)* on the cardiac RyR were more strongly Ca^{2+}-dependent than the effects of either peptide A_S or A_C, with activation being substantially reduced at a *cis* [Ca^{2+}] of only 500 nM (compare Figure 8E with Figures 4E and 7E above).

Actions of peptides *A_S(D-R18)*, A_C and A_S are not additive

To examine the possibility that the cardiac and skeletal *A* peptides were acting at one site, channels were first exposed to 1 μM *A_S(D-R18)*, then 1 μM A_C was added and finally 1 μM A_S (Figure 8F). There was no additive activation by the peptides with either 100 or 500 nM *cis* Ca^{2+}. The voltage-dependent block by peptide A_S at +40 mV occurred when A_S was added in the presence of peptides *A_S(D-R18)* plus A_C.

Peptides *$A_S S$* and *NB* do not activate cardiac RyR channels

In control experiments, peptides *NB* (N-terminal part of the B segment of the skeletal II–III loop) or *$A_S S$* (scrambled peptide A_S

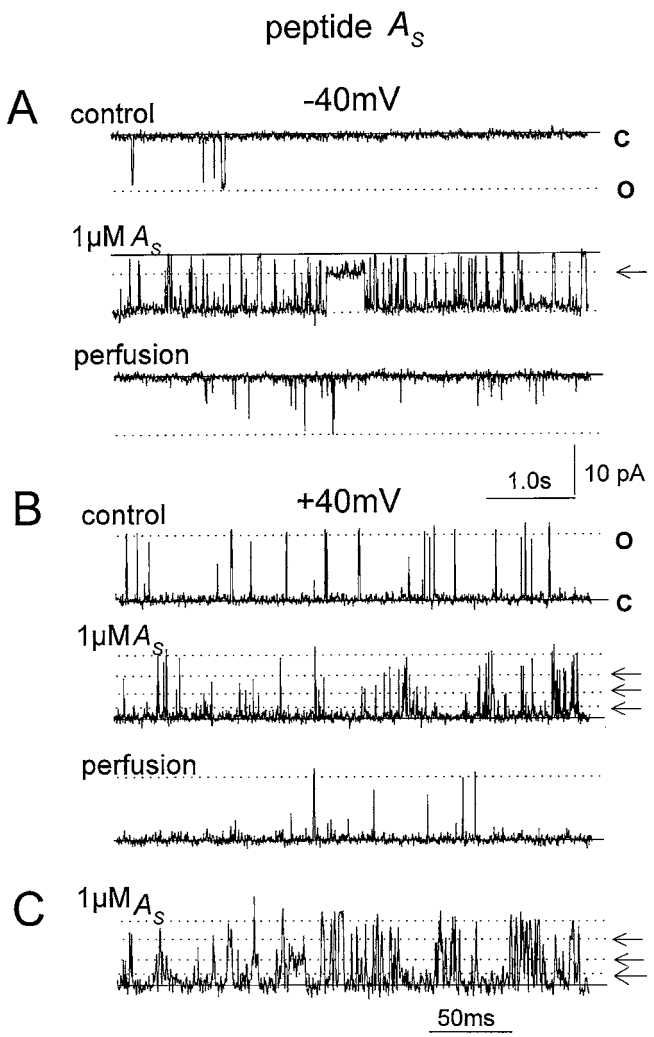

Figure 6 Peptide A_S reversibly activates channels at sub-activating *cis* [Ca^{2+}]

Channel activity at −40 mV is shown in (**A**), and at +40 mV in (**B**). The top traces in (**A**) and (**B**) show control activity with a *cis* [Ca^{2+}] of 100 nM, the second traces show an increase in activity with 1 μM peptide A_S and the third traces recovery after perfusion of the *cis* chamber. There is an increase in submaximal conductance activity (arrows) in the presence of A_S, seen predominantly at +40 mV. The record in (**C**) shows 300 ms of activity with 1 μM peptide A_S at +40 mV with maintained openings to at least three different submaximal conductance levels (arrows). o and c are defined in the legend to Figure 1.

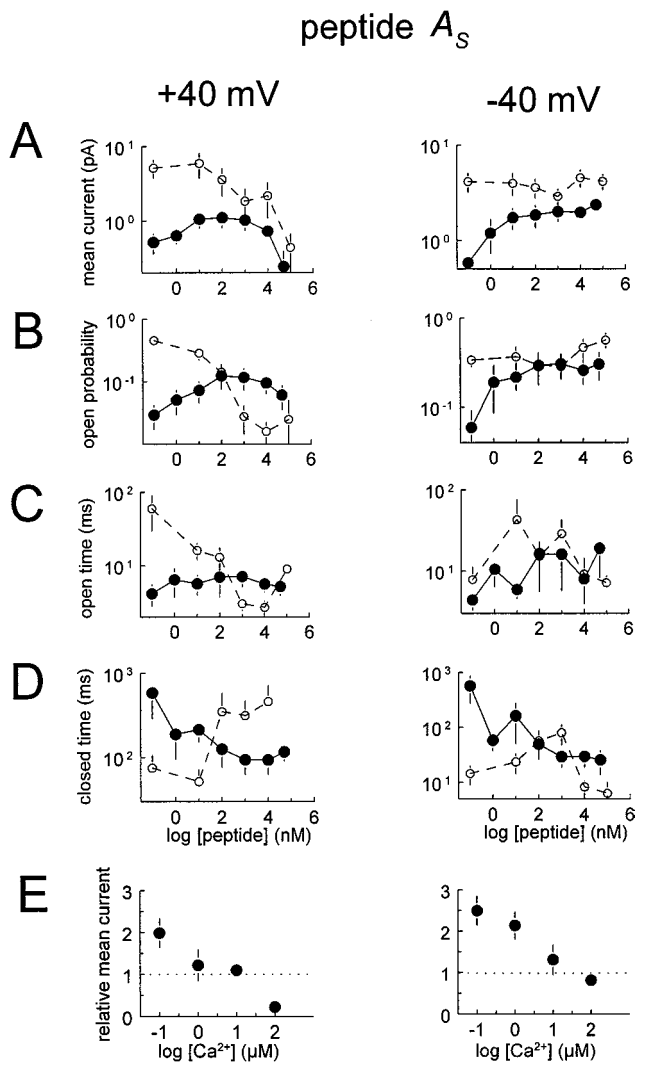

Figure 7 Peptide A_S increases the mean current and open probability of cardiac RyR channels at a sub-activating *cis* [Ca^{2+}] (100 nM), but has little voltage-independent effect on channel activity at 100 μM *cis* Ca^{2+}

●, 100 nM *cis* Ca^{2+}; ○, 100 μM *cis* Ca^{2+}. (**A**)–(**C**) Average parameters as a function of peptide [A_S] (in nM) at +40 mV (left) and −40 mV (right). Data are shown for mean current (**A**), open probability (**B**), mean open time (**C**) and mean closed time (**D**). $n=7$ for all parameters with 100 nM *cis* Ca^{2+}; $n=11$ for average mean current and $n=7$ for single channel parameters with 100 μM *cis* Ca^{2+}. (**E**) Relative mean current as a function of *cis* [Ca^{2+}] in the presence of 1 μM peptide A_S. n for 100 nM and 100 μM Ca^{2+} as above. $n=4$ for 1 μM Ca^{2+} and $n=5$ for 10 μM Ca^{2+}.

sequence) did not activate the cardiac RyR with 100 nM *cis* Ca^{2+} (Table 3). A_SS caused a voltage-dependent block in channel activity at +40 mV. The scrambled peptide caused a similar block of skeletal RyR channels, consistent with the non-specific nature of this action [5].

Peptides A_S and A_S*(D-R18)* enhance Ca^{2+}-induced Ca^{2+} release from cardiac SR

The A_S peptides caused a small increase in resting Ca^{2+} release from cardiac SR, and a substantial increase in both caffeine and Ca^{2+}-induced Ca^{2+} release (Figure 9B). Resting Ca^{2+} release with vehicle alone had a small negative slope, because release is expressed as the rate of release after peptide/vehicle addition (Figure 9A, slope b) minus the preceding rate with thapsigargin (Figure 9A, slope a).

Two additional mutant A_S peptides, A_S2 (Ser-687 → Ala) and A_S2*(D-R18)* (Ser-687 → Ala; with the D isomer of Arg-688), activate skeletal RyR1 and enhance resting Ca^{2+} release from skeletal SR with an efficiency of $A_S < A_S2 < A_S$*(D-R18)* $< A_S2$*(D-R18)* [6,19]. Differential activation of cardiac RyRs was seen in resting Ca^{2+} release, which tended to be greater with A_S*(D-R18)* and A_S2*(D-R18)* than with the other peptides (Figure 9). The peptides each had a similar action on activated Ca^{2+} release, possibly because RyR channels were close to maximally activated under these conditions. Peptide A_S2*(D-R18)* had no effect on the rate of Ca^{2+} uptake by cardiac SR (Figure 9C). Similar results were obtained with peptide A_S ($n=5$) and peptide A_S2 ($n=5$).

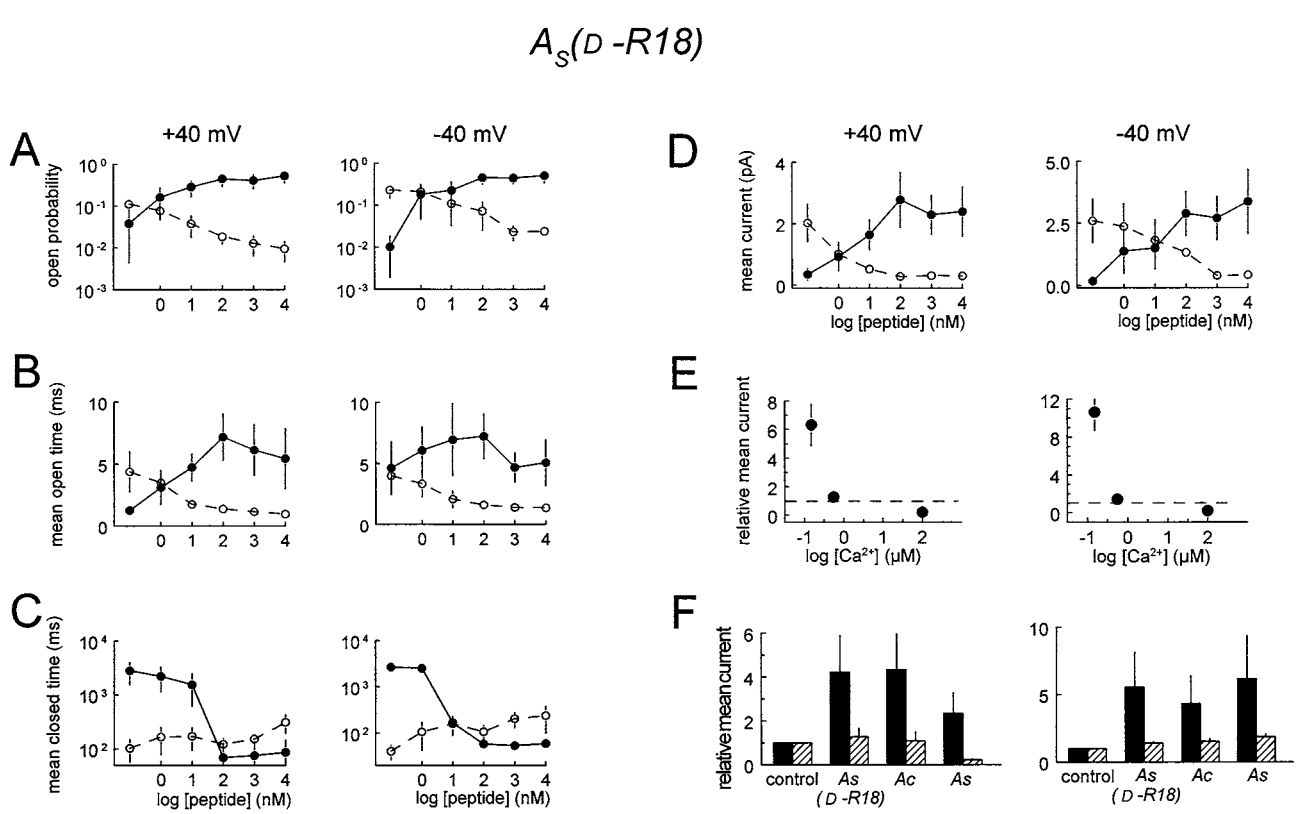

Figure 8 The modified peptide A_S*(D-R18)* activates cardiac RyR channels at 100 nM *cis* Ca^{2+} (●) but inhibits channels with 100 μM *cis* Ca^{2+} (○)

(**A**)–(**C**) Average channel parameters as a function of peptide [A_S*(D-R18)*] (in nM) at + 40 mV (left) and − 40 mV (right). Average data are shown for mean current in (**A**), for open probability (**B**), mean open time (**C**) and mean closed time (**D**). Seven experiments were analysed for mean current with both 100 nM and 100 μM *cis* Ca^{2+}, while six experiments at each Ca^{2+} concentration were analysed for single-channel measurements. (**E**) *cis* [Ca^{2+}]-dependence of the effects of 1 μM A_S*(D-R18)* on relative mean current, with $n = 11$, 5 and 6 for 100 nM, 500 nM and 100 μM *cis* Ca^{2+} repectively. (**F**) Effects of 100 nM peptide A_S*(D-R18)* on relative mean current and the effects of subsequent additions of 1 μM peptide A_C and then 1 μM peptide A_S. The experiment was repeated with 100 and 500 nM *cis* Ca^{2+} (filled and cross-hatched bars, respectively). Each bar shows the mean of five measurements.

Ca^{2+}-release pathways from cardiac SR

Some Ca^{2+} release evoked by the peptides may have occurred through a RyR-indpendent pathway such as the SR Ca^{2+}-ATPase [25,26]. This seemed unlikely since thapsigargin was present and is likely to inhibit Ca^{2+} back flux. Further, resting Ca^{2+} release was abolished by Ruthenium Red added (i) 3 min after the peptide or (ii) 3 min before the peptide (Table 4).

Similarly, Ca^{2+}-induced Ca^{2+} release can be attributed to RyR activation. Adding Ruthenium Red 3 min before Ca^{2+} prevented Ca^{2+} release in response to 20 μM Ca^{2+} alone, or 20 μM Ca^{2+} plus peptide A_S (Table 4). A small Ca^{2+} release with 20 μM Ca^{2+} plus A_S2, A_S*(D-R18)* or A_S2*(D-R18)* was abolished when 30 mM Mg^{2+} was added with thapsigargin to further inhibit the RyR [22].

Effects of [Ca^{2+}] on peptide structure

The Ca^{2+}-dependent actions of the *A* peptides could be due either to an effect of [Ca^{2+}] on peptide structure or on the response of the RyR to the peptide. Therefore, we examined the effect of [Ca^{2+}] on the structure of one of the peptides, A_S*(D-R18)*. The amide region of a series of NOESY (nuclear Overhauser enhancement spectroscopy) spectra are shown in Figure 10. The off-peak diagonals denote amide protons which are close in space

Table 3 Peptides *NB* and $A_S S$ do not alter cardiac RyR activity

Open probability (P_o) is shown at + 40 mV and − 40 mV for individual channels. Means ± S.D. are shown.

	Open probability (P_o)					
	+ 40 mV			− 40 mV		
	Control	1 μM	10 μM	Control	1 μM	10 μM
Peptide $A_S S$ ($n = 11$)	0.037 ± 0.015	0.023 ± 0.007	0.013 ± 0.006	0.028 ± 0.014	0.02 ± 0.008	0.028 ± 0.011
Peptide *NB* ($n = 3$)	0.046 ± 0.016	0.05 ± 0.017	0.054 ± 0.01	0.036 ± 0.013	0.051 ± 0.02	0.040 ± 0.01

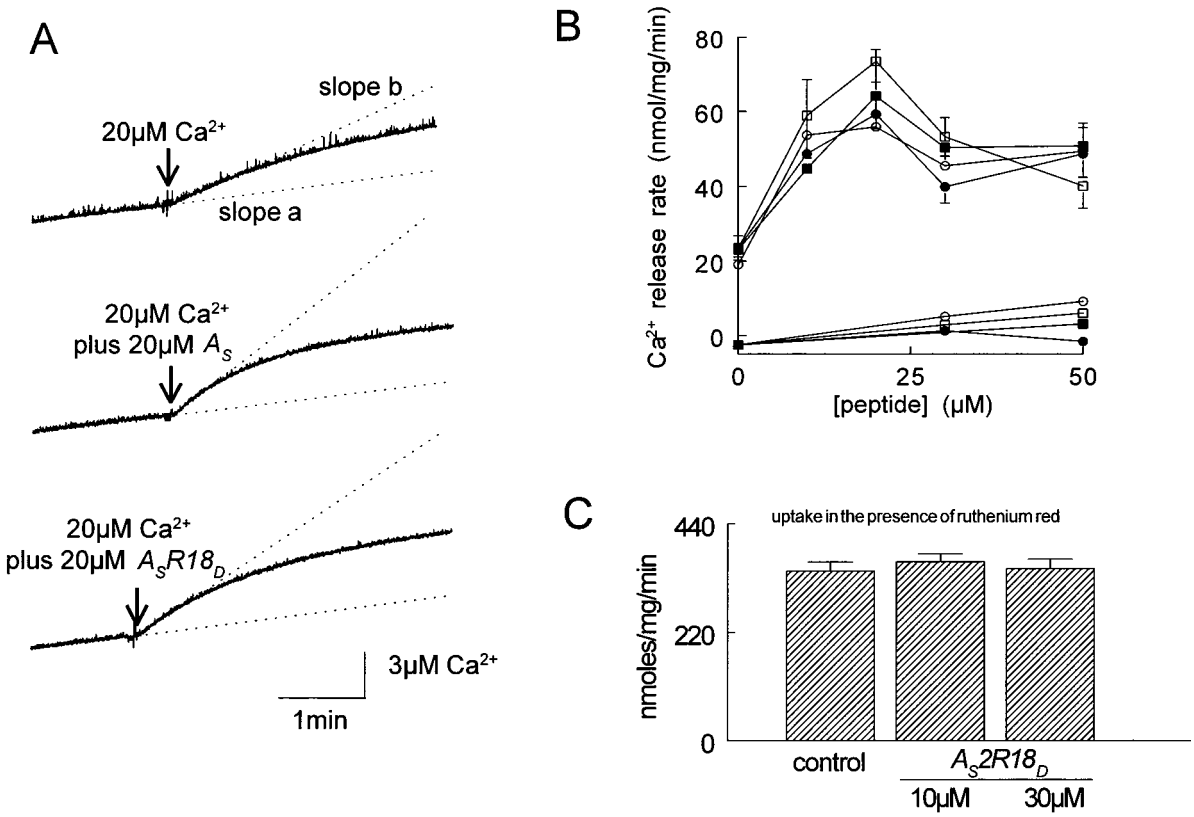

Figure 9 The skeletal *A* peptides, peptide A_S, A_S(D-R18), A_S2 and A_S2(D-R18), increase the rate of resting and Ca^{2+}-induced Ca^{2+} release from cardiac SR vesicles

(**A**) Changes in absorbance, reflecting extravesicular [Ca^{2+}]. The initial part of each record shows resting Ca^{2+} leak in the presence of thapsigargin. The arrow indicates addition of 20 μM Ca^{2+}, either alone (upper) or with A_S (middle) or A_S(D-R18) (lower). A step increase in absorbance with 20 μM Ca^{2+} has been subtracted. Broken lines show the slope with thapsigargin before Ca^{2+}/peptide addition (slope a), and after Ca^{2+}/peptide addition (slope b). (**B**) Average rate of Ca^{2+} release after Ca^{2+}/peptide addition in nmol/mg of protein per min (slope b − slope a). Upper curves show Ca^{2+}-induced Ca^{2+} release (n = 5–9). Lower curves show individual rates of resting Ca^{2+} release, where peptide alone was added 3 min after thapsigargin. Symbols are A_S (●), A_S2 (■), A_S(D-R18) (○) and A_S2(D-R18) (□). Data for caffeine- and Ca^{2+}-induced Ca^{2+} release are grouped together because (i) Ca^{2+} and caffeine act via Ca^{2+} activation [52] and (ii) rates of Ca^{2+} release induced by both 20 μM Ca^{2+} and 2 mM caffeine were between 20 and 30 nmol/mg per min, and there was a similar approx. 3–4-fold increase in the presence of the peptides. (**C**) Effects of A_S2(D-R18) on Ca^{2+} uptake by cardiac SR.

to other amide protons (< 5 Å), indicating that a portion of A_S(D-R18) adopts a helical structure, as reported previously [15]. The number and location of the cross-peaks (Figure 10, arrows) were identical at the different Ca^{2+} concentrations and in the absence of added Ca^{2+}, suggesting that the structure and overall molecular environment of the peptides was similar. The spectra in Figure 10, obtained with the bilayer solution as the peptide vehicle, lacked clarity when compared with spectra obtained with $H_2O/^2H_2O$ (Figure 11) because of the complex ionic conditions.

Comparison of the NOESY spectra of peptides A_C and A_S

The activity of the A_S peptides on skeletal RyRs depends on their α helical structure [15]. Therefore the parallel Ca^{2+}-dependent changes in cardiac RyR activity with the A_C and A_S peptides suggest that the peptides may have structural homology. NOESY spectra show the presence of strong cross-peaks, indicating the presence of α helical regions in both peptides (Figure 11). The first five residues of peptide A_C are similar to the A_S peptide but the rest of the sequence is different, particularly the stretch of glutamate residues located towards the middle of the peptide (see the Experimental section). Nevertheless, the C-terminal half of the peptide contains five basic amino acid residues, and connectivities between the cross-peaks in the NOESY spectrum for A_C (Figure 11) show that these adopt a mostly α-helical conformation. The sequence and conformation of the A_S peptides are important for receptor recognition [20]. Therefore, the ability of the basic residues in peptide A_C to adopt an α-helical conformation may explain the ability of the peptide to interact with the cardiac RyR in a similar manner to the A_S peptides.

DISCUSSION

The results show that peptide fragments with sequences corresponding to the *A* region of the II–III loop of the cardiac and skeletal DHPR alter the activity of native cardiac RyR channels in a Ca^{2+}-dependent manner and alter Ca^{2+} release from cardiac SR. NMR studies show structural similarities between the *A* fragments of the cardiac and skeletal DHPR. The results are consistent with observations that parts of the cardiac and skeletal DHPR bind to the cardiac RyR. Specific functional changes in single cardiac RyR channel activity, induced by binding of fragments of the DHPR, have not been previously reported.

Why have interactions between the skeletal DHPR II–III loop fragments and cardiac RyR channels not been reported previously?

Surface plasmon resonance and two hybrid studies [16,17] indicate that the skeletal DHPR can bind to the cardiac RyR complex.

Table 4 The native II–III loop peptides are ineffective in evoking Ca^{2+} release from the cardiac SR or enhancing Ca^{2+}-induced Ca^{2+} release in the presence of 4 μM Ruthenium Red

Residual Ca^{2+}-induced Ca^{2+} release induced by *A_S2(D-R18)* was blocked by 30 mM Mg^{2+} plus 4 μM Ruthenium Red. The rate of Ca^{2+} release (nmol/mg per min) is the rate after the time at which peptide or toxin is added minus the preceding rate with thapsigargin alone (slope b minus slope a in Figures 5 and 10). Numbers are given as means ± S.E.M. where the number of experiments (*n*) is greater than 3. ND indicates that the experiment was not done.

		Rate of Ca^{2+} release (nmol/mg per min) (*n*)	
Peptide	Peptide concentration (μM)	with Ruthenium Red	with Ruthenium Red plus Mg^{2+}
Resting release			
Control	0	− 2.8 ± 0.21 (6)	ND
A_C	10	− 2.8 (1)	ND
A_S	50	− 3.6 (1)	ND
A_S2	30	− 2.8 (1)	ND
A_S(D-R18)	30	− 1.9 (1)	ND
A_S2(D-R18)	30	− 2.2 (1)	ND
Ca^{2+}-induced Ca^{2+} release			
Control	0	− 0.56 ± 0.16 (6)	− 0.13 (2)
A_C	10	− 0.83 (1)	ND
A_S	50	0.92 (1)	ND
A_S2	30	1.67 (1)	ND
A_S(D-R18)	30	3.33 (1)	ND
A_S2(D-R18)	30	10.8 (1)	− 2.8 (1)
A_S2(D-R18)	10	5.6 (1)	ND

The binding of skeletal II–III loop fragments to the cardiac RyR is not surprising since there is 72% homology between cardiac and skeletal RyRs [27] and 66% homology between cardiac and skeletal DHPRs [28]. In addition, sequences of two skeletal RyR regions that associate with the skeletal DHPR [16,29] are similar in the cardiac RyR. What is surprising is that there are no reports of the functional consequences of this interaction.

The effects on Ca^{2+} release from cardiac SR may not have been seen because the peptides alter this release only (i) during Ca^{2+}-induced Ca^{2+} release and (ii) in the presence of thapsigargin. Previous Ca^{2+} release studies [8,11] were not done under these conditions. The effects on single channel activity may not have been seen because purified cardiac RyR channels were examined at activating *cis* [Ca^{2+}] [12]. The use of higher *cis* [Ca^{2+}] would have reduced the ability of the peptides to enhance channel activity. Furthermore, purification may have altered the ability of channels to respond to DHPR fragments, by either removing an associated protein or by modifying the channel. Proteins that remain associated with the RyR in bilayers include triadin/junctin and calsequestrin [30] as well as FK506-binding proteins, Ca^{2+}/calmodulin kinase II and protein kinase A [31–34]. Therefore some of the interactions described here may depend on, or be modulated by, an associated protein. Indeed, the action of calsequestrin on the RyR is mediated by triadin and junctin [30], while interactions between the skeletal DHPR II–III loop and RyR require FKBP12 [5,35,36].

Can different isoforms of the DHPR and RyR interact?

The results suggest that both the skeletal and cardiac DHPRs have the potential to physically interact with cardiac RyRs. Interactions between the *C* region of the cardiac DHPR II–III loop and skeletal RyR have been reported [6] as has co-immunoprecipitation of the cardiac DHPR and skeletal RyR [37]. If the cardiac DHPR can associate with the skeletal RyR, then why is skeletal EC coupling abolished in dysgenic myocytes transfected with cardiac DHPR [2,38]? It is likely that skeletal EC coupling depends on correct targeting of sufficient numbers of DHPRs into tetrads located directly opposite RyRs [39]. Similarly the skeletal RyR may be a co-requisite for correct targeting of the DHPR into tetrads, and for appropriate transmission of the EC coupling signal through the RyR to the channel gating mechanism [40].

Is there a physical interaction between the DHPR and RyR in the heart?

The *A* region of the skeletal DHPR appears not to be directly involved in skeletal EC coupling [1–3], and its role in the interaction between the skeletal DHPR and RyR remains uncertain [3]. Nevertheless the present results revive the possibility that there is a physical association between the DHPR and RyR in cardiac muscle [18,41]. DHPRs do not form tetrads in the heart [42] and the DHPR/RyR ratio is lower than in skeletal muscle [43], therefore only a few RyRs could be physically associated with DHPRs. Depolarization-induced conformational coupling in the heart is supported by some studies [44], but not others [45] and not generally thought to contribute to EC coupling [46]. However, an association between the proteins could allow the DHPR to modulate EC coupling and/or resting Ca^{2+} release under some conditions.

Voltage-dependent and -independent interactions between the peptides and the cardiac RyR

The different actions of the peptides are likely to reflect peptide binding to at least two different sites on the RyR complex. The voltage-dependent (Ca^{2+}-independent) block by A_S is attributed to an interaction between positively charged residues in the peptide and negatively charged residues in the pore [5] and is observed with other basic peptides which also block K^+ channels [47]. In contrast the voltage-independent effects are due to peptide binding to a region that is not influenced by membrane field. It is likely that voltage-independent effects were induced by peptides *A_S(D-R18)*, A_C and A_S binding to the same site on the RyR given their structural similarity, their similar Ca^{2+} dependence and the non-additive nature of their effects. Since the peptide structure was not influenced by [Ca^{2+}], either (i) the RyR's response to peptide binding to one site is Ca^{2+}-dependent, or (ii) different binding sites are available at sub-activating and activating [Ca^{2+}]. The experiments did not distinguish between these possibilities.

It was not surprising that voltage-dependent block was seen only with peptide A_S because the low positive charge density on peptide A_C [48] would reduce its capacity to interact with acidic pore residues, while the structured nature of *A_S(D-R18)* [15] would prevent it from blocking the pore (since the *A* peptides block with lower efficacy as peptide structure increases [19]).

Effects of the *A* peptides on RyR channels and Ca^{2+} release from cardiac SR

Effects of the *A* peptides on Ca^{2+} release from SR confirmed the interaction between the peptides and the Ca^{2+}-release channel. Peptide A_C had a similar action in the bilayer and Ca^{2+}-release experiments. The peptide increased RyR activity in bilayers in the presence of 100 nM Ca^{2+}, had little effect at 1 μM Ca^{2+} and depressed activity with 10 and 100 μM Ca^{2+}. There was no effect on resting Ca^{2+} release in the presence of thapsigargin, where Ca^{2+} leak from the vesicles raised extravesicular [Ca^{2+}] to approx.

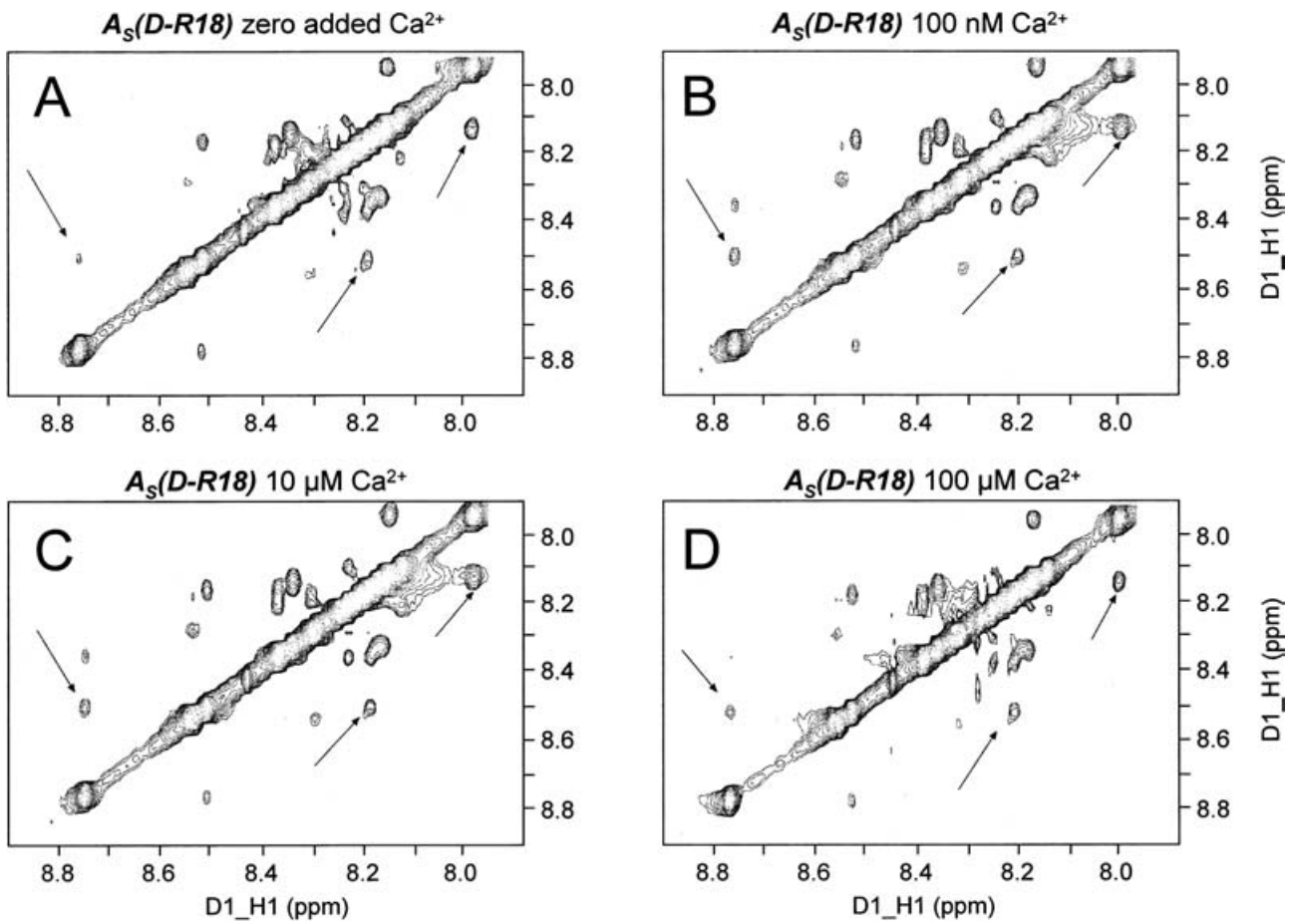

Figure 10 Ca^{2+} concentration does not alter the structure of peptide A_S(D-R18)

NOESY spectra of the amide region of the A_S(D-R18) peptide (2 mM) are shown. The peptide was dissolved in the *cis* solution containing: 230 mM caesium methanesulphonate, 20 mM CsCl and 10 mM Tes (pH 7.4 with CsOH). Ca^{2+} was buffered with 1 mM BAPTA in the 100 nM and 10 μM Ca^{2+} solutions. Spectra are shown with no added Ca^{2+} (**A**), 100 nM Ca^{2+} (**B**), 10 μM Ca^{2+} (**C**) and 100 μM Ca^{2+} (**D**). The arrows show examples of off-peak diagonals, which indicate amide-amide interactions at distance of less than 5 Å in an α-helical structure. Changes in the position of the off-peak diagonals would have been indicative of Ca^{2+}-dependent structural changes in the peptide.

1 μM. However Ca^{2+} release in the presence of 20 μM Ca^{2+} was depressed.

The effects of the skeletal A_S peptides were also similar in the bilayer and Ca^{2+}-release experiments in that activation was seen in both cases. However, in this case, although the peptides enhanced channel activity less at higher Ca^{2+} concentrations, Ca^{2+}-induced Ca^{2+} release was potentiated more than resting Ca^{2+} release. Thus the Ca^{2+} concentration dependence of the *A* peptide's action was different in the bilayer and Ca^{2+}-release experiments. Since the transition between activation and inhibition occurred at approx. 10 μM *cis* Ca^{2+}, only a small shift in the Ca^{2+}-dependence could explain the results.

Although skeletal and cardiac RyR channels in bilayers are similarly sensitive to the A_S peptides, Ca^{2+} release from cardiac SR is less sensitive to the peptides than release from skeletal SR [5]. It is possible that peptide concentrations could not be increased sufficiently to enhance Ca^{2+} release, since more peptide is required to induce Ca^{2+} release than to activate channels in bilayers [5,35,49]. The properties of channels in bilayers may differ from those in vesicles, perhaps because of the infiltration of non-native lipids in the bilayer system or because of the different ionic conditions or the presence of antipyralazo in the Ca^{2+} release experiments. However, since peptides A_S and A_S(D-R18) increase resting Ca^{2+} efflux from skeletal SR under our conditions [5,15], cardiac channels appear to be more sensitive to differences between the techniques.

A peptide corresponding to the C-terminal 10 residues of A_C reduces Ca^{2+} spark frequency in cardiac myocytes [18], whereas the full peptide A_C enhanced cardiac RyRs in bilayers with a resting [Ca^{2+}] of 100 nM. The different-length peptides may have slightly different actions on the RyR. However, the results can be explained if the [Ca^{2+}] near the RyR channel at the time of spark initiation is >100 nM. The [Ca^{2+}] near the channel is greater than in the bulk solution, because of Ca^{2+} leak through the pore from the luminal store or Ca^{2+} entry through nearby L-type Ca^{2+} channels [50,51]. A Ca^{2+} spark occurs when local increases in [Ca^{2+}] initiate Ca^{2+}-induced Ca^{2+} release. Thus, with Ca^{2+} near the pore well in excess of 100 nM before spark initiation, we would predict that peptide A_C would reduce the probability of the RyR opening and spark generation.

In conclusion, we show functional interactions between the cardiac RyR and the *A* region of both the cardiac and skeletal DHPR. This study supports the possibility that DHPR can become physically coupled (either directly or through associated proteins) to cardiac RyRs in the myocardium. Such coupling is clearly not the mechanism for cardiac EC coupling, but could have other

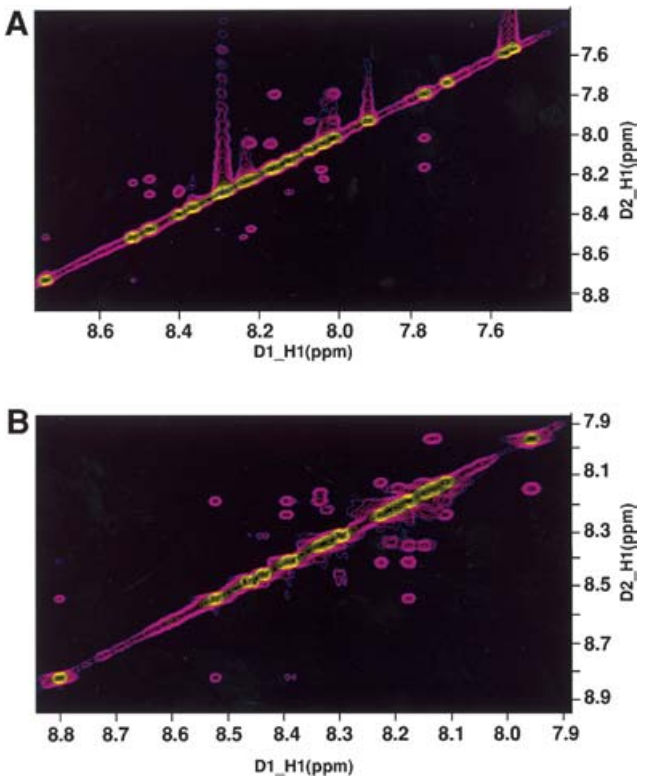

Figure 11 A_C **peptide contains significant helical structure**

The amide portion of the ^{1}H NOESY spectra showing amide–amide connectivities for peptides A_C (in **A**) and A_S (in **B**) using $^2H_2O/H_2O$ vehicle (see the Experimental section). These off-peak diagonals are indicative of a helical structure.

functional implications which require further investigation. The results show that the cardiac and skeletal *A* region peptides can be used as probes for cardiac and skeletal RyR channel activity.

We are grateful to Suzy Pace and Joan Stivala for assistance with SR vesicle preparation and characterization. The work was supported by grants form the National Heart Foundation of Australian (no. G 01C 0296) and the National Health and Medical Research Council (no. 224235).

REFERENCES

1 Tanabe, T., Beam, K. G., Powell, J. A. and Numa, S. (1988) Restoration of excitation-contraction coupling and slow calcium current in dysgenic muscle by dihydropyridine receptor complementary DNA. Nature (London) **336**, 134–139
2 Wilkens, C. M., Kasielke, N., Flucher, B. E., Beam, K. G. and Grabner, M. (2001) Excitation-contraction coupling is unaffected by drastic alteration of the sequence surrounding residues L720-L764 of the alpha 1S II-III loop. Proc. Natl. Acad. Sci. U.S.A. **98**, 5892–5897
3 Ahern, C. A., Bhattacharya, D., Mortenson, L. and Coronado, R. (2001) A component of excitation-contraction coupling triggered in the absence of the T671-L690 and L720-Q765 regions of the II-III loop of the dihydropyridine receptor alpha(1s) pore subunit. Biophys. J. **81**, 3294–3307
4 Xu, L., Tripathy, A., Pasek, D. A. and Meissner, G. (1998) Potential for Pharmacology of ryanodine receptor/calcium release channels. Ann. N.Y. Acad. Sci. **853**, 130–148
5 Dulhunty, A. F., Laver, D. R., Gallant, E. M., Casarotto, M. G., Pace, S. M. and Curtis, S. (1999) Activation and inhibition of skeletal RyR channels by a part of the skeletal DHPR II-III loop: effects of DHPR Ser687 and FKBP12. Biophys. J. **77**, 189–203
6 Dulhunty, A. F., Haarmann, C., Green, D., Laver, D. R., Board, P. G. and Casarotto, M. G. (2002) Interactions between dihydropyridine receptors and ryanodine receptors in striated muscle. Prog. Biophys. Mol. Biol. **79**, 45–75
7 Gallant, E. M., Curtis, S., Pace, S. M. and Dulhunty, A. F. (2001) Arg(615)Cys substitution in pig skeletal ryanodine receptors increases activation of single channels by a segment of the skeletal DHPR II-III loop. Biophys. J. **80**, 1769–1782
8 Yamamoto, T., Rodriguez, J. and Ikemoto, N. (2002) Ca^{2+}-dependent dual functions of peptide C. The peptide corresponding to the Glu724-Pro760 region (the so-called determinant of excitation-contraction coupling) of the dihydropyridine receptor alpha 1 subunit II-III loop. J. Biol. Chem. **277**, 993–1001
9 Haarmann, C. C., Green, D., Casarotto, M. G., Laver, D. R. and Dulhunty, A. F. (2003) The random-coil 'C' fragment of the dihydropyridine receptor II–III loop can activate or inhibit native skeletal ryanodine receptors. Biochem. J. **372**, 305–316
10 Chen, L., Esteve, E., Sabatier, J. M., Ronjat, M., De Waard, M., Allen, P. D. and Pessah, I. N. (2003) Maurocalcine and peptide A stabilize distinct subconductance states of ryanodine receptor type 1, revealing a proportional gating mechanism. J. Biol. Chem. **278**, 16095–16106
11 El-Hayek, R., Antoniu, B., Wang, J., Hamilton, S. L. and Ikemoto, N. (1995) Identification of calcium release-triggering and blocking regions of the II-III loop of the skeletal muscle dihydropyridine receptor. J. Biol. Chem. **270**, 22116–22118
12 Stange, M., Tripathy, A. and Meissner, G. (2001) Two domains in dihydropyridine receptor activate the skeletal muscle Ca^{2+} release channel. Biophys. J. **81**, 1419–1429
13 Tripathy, A., Resch, W., Xu, L., Valdivia, H. H. and Meissner, G. (1998) Imperatoxin A induces subconductance states in Ca^{2+} release channels (ryanodine receptors) of cardiac and skeletal muscle. J. Gen. Physiol. **111**, 679–690
14 Gurrola, G. B., Arevalo, C., Sreekumar, R., Lokuta, A. J., Walker, J. W. and Valdivia, H. H. (1999) Activation of ryanodine receptors by imperatoxin A and a peptide segment of the II-III loop of the dihydropyridine receptor. J. Biol. Chem. **274**, 7879–7886
15 Green, D., Pace, S., Curtis, S. M., Sakowska, M., Lamb, G. D., Dulhunty, A. F. and Casarotto, M. G. (2003) The three-dimensional structural surface of two beta-sheet scorpion toxins mimics that of an alpha-helical dihydropyridine receptor segment. Biochem. J. **370**, 517–527
16 Proenza, C., O'Brien, J., Nakai, J., Mukherjee, S., Allen, P. D. and Beam, K. G. (2002) Identification of a region of RyR1 that participates in allosteric coupling with the alpha(1S) (Ca(V)1.1) II-III loop. J. Biol. Chem. **277**, 6530–6535
17 O'Reilly, F. M. and Ronjat, M. (1999) Direct interaction of the skeletal dihydropyridine receptor alpha 1 subunit with skeletal and cardiac ryanodine receptors. Biophys. J. **76**, A466
18 Li, Y. and Bers, D. M. (2001) A cardiac dihydropyridine receptor II-III loop peptide inhibits resting Ca^{2+} sparks in ferret ventricular myocytes. J. Physiol. **537**, 17–26
19 Casarotto, M. G., Gibson, F., Pace, S. M., Curtis, S. M., Mulcair, M. and Dulhunty, A. F. (2000) A structural requirement for activation of skeletal ryanodine receptors by peptides of the dihydropyridine receptor II-III loop. J. Biol. Chem. **275**, 11631–11637
20 Casarotto, M. G., Green, D., Pace, S. M., Curtis, S. M. and Dulhunty, A. F. (2001) Structural determinants for activation or inhibition of ryanodine receptors by basic residues in the dihydropyridine receptor II-III loop. Biophys. J. **80**, 2715–2726
21 Chamberlain, B. K. and Fleischer, S. (1988) Isolation of canine cardiac sarcoplasmic reticulum. Methods Enzymol. **157**, 91–99
22 Laver, D. R., Baynes, T. M. and Dulhunty, A. F. (1997) Magnesium inhibition of ryanodine-receptor calcium channels: evidence for two independent mechanisms. J. Membr. Biol. **156**, 213–229
23 King, B. M. and Bear, G. (1993) Some (almost) assumption-free tests. In Statistical Reasoning in Psycology and Education (Minium, E. W., ed.), pp. 474–496, Wiley, New York
24 Xu, L., Mann, G. and Meissner, G. (1996) Regulation of cardiac Ca^{2+} release channel (ryanodine receptor) by Ca^{2+}, H^+, Mg^{2+}, and adenine nucleotides under normal and simulated ischemic conditions. Circ. Res. **79**, 1100–1109
25 Shannon, T. R., Ginsburg, K. S. and Bers, D. M. (2002) Quantitative assessment of the SR Ca^{2+} leak-load relationship. Circ. Res. **91**, 594–600
26 Macdonald, W. A. and Stephenson, D. G. (2001) Effects of ADP on sarcoplasmic reticulum function in mechanically skinned skeletal muscle fibres of the rat. J. Physiol. **532**, 499–508
27 Otsu, K., Willard, H. F., Khanna, V. K., Zorzato, F., Green, N. M. and Maclennan, D. H. (1990) Molecular cloning of cDNA encoding the Ca^{++} release channel (ryanodine receptor) of rabbit cardiac muscle sarcoplasmic reticulum. J. Biol. Chem. **265**, 13472–13483
28 Mikami, A., Imoto, K., Tanabe, T., Niidome, T., Mori, Y., Takeshima, H., Narumiya, S. and Numa, S. (1989) Primary structure and functional expression of the cardiac dihydropyridine-sensitive calcium channel. Nature (London) **340**, 230–233
29 Leong, P. and MacLennan, D. H. (1998) A 37-amino acid sequence in the skeletal muscle ryanodine receptor interacts with the cytoplasmic loop between domains II and III in the skeletal muscle dihydropyridine receptor. J. Biol. Chem. **273**, 7791–7794

30 Beard, N. A., Sakowska, M. M., Dulhunty, A. F. and Laver, D. R. (2002) Calsequestrin is an inhibitor of skeletal muscle ryanodine receptor calcium release channels. Biophys. J. **82**, 310–320
31 Ahern, G. P., Junankar, P. R. and Dulhunty, A. F. (1994) Single channel activity of the ryanodine receptor calcium release channel is modulated by FK-506. FEBS Lett. **352**, 369–374
32 Marx, S. O., Gaburjakova, J., Gaburjakova, M., Henrikson, C., Ondrias, K. and Marks, A. R. (2001) Coupled gating between cardiac calcium release channels (ryanodine receptors). Circ. Res. **88**, 1151–1158
33 Marx, S. O., Reiken, S., Hisamatsu, Y., Jayaraman, T., Burkhoff, D., Rosemblit, N. and Marks, A. R. (2000) PKA phosphorylation dissociates FKBP12.6 from the calcium release channel (ryanodine receptor): defective regulation in failing hearts. Cell **101**, 365–376
34 Dulhunty, A. F., Laver, D., Curtis, S. M., Pace, S., Haarmann, C. and Gallant, E. M. (2001) Characteristics of irreversible ATP activation suggest that native skeletal ryanodine receptors can be phosphorylated via an endogenous CaMKII. Biophys. J. **81**, 3240–3252
35 Lamb, G. D., El-Hayek, R., Ikemoto, N. and Stephenson, D. G. (2001) Effects of dihydropyridine receptor II-III loop peptides on Ca^{2+} release in skinned skeletal muscle fibers. Am. J. Physiol. **279**, C891–C905
36 O'Reilly, F. M., Robert, M., Jona, I., Szegedi, C., Albrieux, M., Geib, S., De Waard, M., Villaz, M. and Ronjat, M. (2002) FKBP12 modulation of the binding of the skeletal ryanodine receptor onto the II-III loop of the dihydropyridine receptor. Biophys. J. **82**, 145–155
37 Mouton, J., Marty, I., Villaz, M., Feltz, A. and Maulet, Y. (2001) Molecular interaction of dihydropyridine receptors with type-1 ryanodine receptors in rat brain. Biochem. J. **354**, 597–603
38 Nakai, J., Tanabe, T., Konno, T., Adams, B. and Beam, K. G. (1998) Localization in the II-III loop of the dihydropyridine receptor of a sequence critical for excitation-contraction coupling. J. Biol. Chem. **273**, 24983–24986
39 Flucher, B. E. (2001) Molecular structure and assembly of the function of the calcium release units in skeletal muscle. Proc. Int. Union Physiol. Sci. XXXIV, abstract 2942
40 Nakai, J., Ogura, T., Protasi, F., Franzini-Armstrong, C., Allen, P. D. and Beam, K. G. (1997) Functional nonequality of the cardiac and skeletal ryanodine receptors. Proc. Natl. Acad. Sci. U.S.A. **94**, 1019–1022
41 Katoh, H., Schlotthauer, K. and Bers, D. M. (2000) Transmission of information from cardiac dihydropyridine receptor to ryanodine receptor: evidence from BayK 8644 effects on resting Ca^{2+} sparks. Circ. Res. **87**, 106–111
42 Franzini-Armstrong, C., Protasi, F. and Ramesh, V. (1998) Comparative ultrastructure of Ca^{2+} release units in skeletal and cardiac muscle. Ann. N.Y. Acad. Sci. **853**, 20–30
43 Bers, D. M. and Stiffel, V. M. (1993) Ratio of ryanodine to dihydropyridine receptors in cardiac and skeletal muscle and implications for E-C coupling. Am. J. Physiol. **264**, C1587–C1593
44 Howlett, S. E., Zhu, J. Q. and Ferrier, G. R. (1998) Contribution of a voltage-sensitive calcium release mechanism to contraction in cardiac ventricular myocytes. Am. J. Physiol. **274**, H155–H170
45 Piacentino, V., 3rd, Dipla, K., Gaughan, J. P. and Houser, S. R. (2000) Voltage-dependent Ca^{2+} release from the SR of feline ventricular myocytes is explained by Ca^{2+}-induced Ca^{2+} release. J. Physiol. **523**, 533–548
46 Wier, W. G. and Balke, C. W. (1999) Ca^{2+} release mechanisms, Ca^{2+} sparks, and local control of excitation-contraction coupling in normal heart muscle. Circ. Res. **85**, 770–776
47 Mead, F. C., Sullivan, D. and Williams, A. J. (1998) Evidence for negative charge in the conduction pathway of the cardiac ryanodine receptor channel provided by the interaction of K^+ channel N-type inactivation peptides. J. Membr. Biol. **163**, 225–234
48 Zhu, X., Gurrola, G., Jiang, M. T., Walker, J. W. and Valdivia, H. H. (1999) Conversion of an inactive cardiac dihydropyridine receptor II-III loop segment into forms that activate skeletal ryanodine receptors. FEBS Lett. **450**, 221–226
49 Lu, X., Xu, L. and Meissner, G. (1994) Activation of the skeletal muscle calcium release channel by a cytoplasmic loop of the dihydropyridine receptor. J. Biol. Chem. **269**, 6511–6516
50 Satoh, H., Blatter, L. A. and Bers, D. M. (1997) Effects of $[Ca^{2+}]_i$, SR Ca^{2+} load, and rest on Ca^{2+} spark frequency in ventricular myocytes. Am. J. Physiol. **272**, H657–H668
51 Wang, S. Q., Song, L. S., Lakatta, E. G. and Cheng, H. (2001) Ca^{2+} signalling between single L-type Ca^{2+} channels and ryanodine receptors in heart cells. Nature (London) **410**, 592–596
52 Sitsapesan, R. and Williams, A. J. (1990) Mechanisms of caffeine activation of single calcium-release channels of sheep cardiac sarcoplasmic reticulum. J. Physiol. **423**, 425–439

Received 22 July 2003/13 November 2003; accepted 16 December 2003
Published as BJ Immediate Publication 16 December 2003, DOI 10.1042/BJ20031096